FEBS Letters 588 (2014) 2859–2866

journal homepage: www.FEBSLetters.org

FERM domain-containing unconventional myosin VIIA interacts with integrin β5 subunit and regulates αvβ5-mediated cell adhesion and migration

Yuqing Liu, Lizhao Guan, Jun Zhan, Danyu Lu, Junhu Wan, Hongquan Zhang *

Key Laboratory of Carcinogenesis and Translational Research, Ministry of Education, Peking University Health Science Center, Beijing 100191, China
State Key Laboratory of Natural and Biomimetic Drugs, Peking University Health Science Center, Beijing 100191, China
Laboratory of Molecular Cell Biology and Tumor Biology, Department of Anatomy, Histology and Embryology, Peking University Health Science Center, Beijing 100191, China

ARTICLE INFO

Article history:
Received 16 April 2014
Revised 16 June 2014
Accepted 17 June 2014
Available online 2 July 2014

Edited by Dietmar J. Manstein

Keywords:
Myosin VIIA
Integrin β5 subunit
Cell adhesion
Cell migration
Hereditary deafness

ABSTRACT

Unconventional myosin VIIA (Myo7a) has been known to associate with hereditary deafness. Here we present a novel function of Myo7a by identifying that Myo7a directly interacts with integrin β5 subunit and regulates cell adhesion and motility in an integrin-dependent manner. We found that Myo7a bound to the cytoplasmic tail of integrin β5. Further, we pinpointed an integrin-binding domain at F3 of the first FERM domain and F1 of the second FERM domain. Functionally, Myo7a-induced cell adhesion and migration were mediated by integrin αvβ5. These findings indicated that Myo7a interacts with integrin β5 and selectively promotes integrin αvβ5-mediated cell migration.

Structured summary of protein interactions:
integrin B5 physically interacts with **Myo7a** by pull down (1, 2, 3, 4, 5, 6)
Myo7a binds to **integrin B5** by pull down (1, 2)
integrinB5 physically interacts with **Myo7a** by anti bait coip (1, 2, 3)

1. Introduction

Integrins, as heterodimeric transmembrane receptors, mediate interactions between cells and extracellular matrix (ECM) and are involved in cell adhesion and migration [1]. Integrins are composed of α and β subunits, 18 α and 8 β subunits form 24 distinct integrin hetrodimers [2]. Integrin α and β subunit both contain a large N-terminal extracellular domain, a single transmembrane domain and a short C-terminal cytoplasmic tail. Integrins regulate the binding affinity with ECM through an inside-out signaling and control cell migration via an outside-in signaling [1]. Unconventional myosins are a superfamily of actin-based motor proteins implicated in diverse cellular processes, including cytokinesis, pseudopod extension, vesicle transport and phagocytosis [3,4]. As a member of them, myosin VIIA (Myo7a) is mainly expressed in the stereocilia in the inner ear and is required for the maintenance of the structure of stereocilia. Increasing evidence has suggested that Myo7a associate with hereditary hearing loss. Mutations in *MYO7A* cause syndromic (USH1B) [5] and non-syndromic (DFNB2 and DFNA11) [6,7] deafness in humans, and are also responsible for the phenotype of shaker-1 mice [8].

Structurally, unconventional myosins are composed of a conserved motor head, a neck region and a variable tail. It is known that the tails differ extremely in length and domain composition among myosin family members, which determines the cellular localization and function of the myosin. Notably, the tail of Myo7a contains several domains, including two FERM domains. Each FERM domain typically is composed of F1, F2 and F3 lobes, which interact directly or indirectly with multiple integral membrane proteins, link the cytoskeleton to the plasma membrane, and thus participate in a variety of cellular functions, such as the regulation of cell extension and polarity, cell migration, etc. [9,10]. Talin, a FERM-containing protein, has been reported to bind to integrin β subunit tail through its F2 and F3 subdomains and therefore activates integrins [11]. Kindlin-2, another FERM domain-containing protein that activates integrins, also interacts with integrin β

* Corresponding author at: Laboratory of Molecular Cell Biology and Tumor Biology, Department of Histology and Embryology, School of Basic Medical Sciences, Peking University Health Science Center, #38 Xue Yuan Road, Beijing 100191, China.
E-mail address: Hongquan.Zhang@bjmu.edu.cn (H. Zhang).

http://dx.doi.org/10.1016/j.febslet.2014.06.049
0014-5793/

subunit tail via its FERM domain [12]. Interestingly, we previously found that unconventional Myo10 interacts with integrin β cytoplasmic domain and regulates integrin transport within filopodia via the lobes F2 and F3 of its FERM domain [13]. Thus, we proposed a hypothesis that Myo7a may also interact with integrin cytoplasmic domain and plays a role in integrin-mediated cellular functions such as cell adhesion and migration. Here, we identified that Myo7a directly interacted with integrin β5 cytoplasmic domain. Furthermore, the roles of Myo7a in integrin β5-mediated cellular functions were examined in non-stereocilia cells. Taken together, we present the first report that Myo7a regulates cell adhesion and migration in non-stereocilia cells by association with integrin αvβ5.

2. Materials and methods

2.1. Cell lines

African green monkey kidney COS-7 cells, human embryonic kidney 293T cells and human breast cancer MCF-7 cells were cultured in DMEM medium (Invitrogen, Carlsbad, CA) and mouse melanoma B16 cells were cultured in RPMI 1640 medium (Invitrogen, Carlsbad, CA). Both culture mediums were supplemented with 10% fetal bovine serum (FBS) (Invitrogen, Carlsbad, CA), 100 IU/ml of penicillin and 100 μg/ml of streptomycin respectively. The cells were cultured at 37 °C with 5% CO_2 in a humidified incubator.

2.2. cDNA expression vectors

GST-integrin β1, GST-integrin β3 and GST-integrin β5 cytoplasmic domain fusion protein expression vectors were kindly provided by Dr. Staffan Strömblad (Karolinska Institutet, Sweden) [14]. A full-length mouse GFP-Myo7a plasmid (Accession No. AY821853) was kindly provided by Dr. Thomas B. Friedman (National Institute of Health, USA) [15]. A full-length Myo7a ORF was excised from the GFP-Myo7a plasmid with EcoRI/SalI restriction enzymes, filled in 5′-protruding ends using DNA polymerase I large (Klenow) fragment (Promega, Madison, WI, USA), and cloned in-frame into the EcoRI/EcoRV sites of a mutant p3 × Flag-CMV 10 vector with a G inserted ahead of EcoRI site to generate plasmid Flag-Myo7a. The Flag-tagged, GFP-tagged and MBP-tagged Myo7a fragments were all PCR amplified from GFP-Myo7a plasmid, and cloned in-frame into the mutant p3 × Flag-CMV 10 vector, pEGFP-C2 vector and pMal-C2 vector respectively. All the primers used were listed in Supplementary Table 1.

2.3. Western blot assays

Cell lysates were prepared using PBSTDS lysis buffer (0.01 M PBS, 1% Triton X-100, 5 g/L Sodium deoxycholate, 0.1% SDS and 1 mM EDTA) containing cocktail protease inhibitor (Boehringer Mannheim, Mannheim, Germany). Proteins were denatured at 95 °C for 5 min and then separated by SDS–PAGE. Separated proteins were transferred to PVDF membranes (Millipore, Billerica, MA) following blocked by 5% milk in TBS-Tween-20 buffer for 1 h and incubated with anti-Myo7a antibody (ab3481, Abcam, Cambridge, MA), anti-Flag (F3165, Sigma–Aldrich, St. Louis, MO), anti-integrin β5 (D24A5, Cell Signaling Technology, Danvers, MA), anti-GFP antibody (MAB 1083, Millipore, Darmstadt, Germany) or anti-β-actin (TA-09, Zhongshan golden bridge, Beijing, China) overnight at 4 °C. After washing for 3 times in TBS buffer, the membranes were incubated with HRP-conjugated secondary antibody for 1 h at room temperature. The signal was detected using a chemiluminescence detection kit (Pierce, Rockford, IL).

2.4. Purification of fusion proteins and GST pull-down assays

GST, GST-integrin β1, GST-integrin β3 or GST-integrin β5 and MBP, MBP-Myo7a FERM-1or MBP-Myo7a FERM-2 were expressed in *Escherichia coli* BL_{21} (Tiangen Biotechnology, Beijing, China), and purified with Glutathione Sepharose 4B beads (Pharmacia Medtech, Piscataway, NJ) or MBP-Affinity Matrix (Amylose Resin, New England Biolabs). GST/MBP pull-down assays were performed as described previously [16]. Briefly, GST or GST-fusion protein was incubated with Glutathione Sepharose 4B beads by rocking at 4 °C for 4 h, and then the beads were washed three times with TEN buffer (20 mM Tris–HCl, pH 7.4, 0.1 mM EDTA, and 100 mM NaCl) followed by incubating with pre-cleared lysates overnight at 4 °C. And the beads were dissolved into 2 × SDS loading buffer after centrifugation, and boiled 5 min at 100 °C.

2.5. Co-immunoprecipitation (Co-IP)

A Co-IP assay was performed as described previously [16]. Briefly, B16 cells were transfected with pFlag-Myo7a tail by Lipofectamine 2000 (Invitrogen, Carlsbad, CA). Total cell lysates were extracted using RIPA buffer (1 × PBS, pH 7.4, 0.5% sodium deoxycholate, 1% Triton X-100, 0.1% SDS) with cocktail protease inhibitors. Approximately 500 μg of pre-cleared lysates were immunoprecipitated by specific antibodies with constant rotation overnight at 4 °C. Protein A agarose beads were then added and incubated for another 2 h. Then the beads were washed three times using the lysis buffer. 2 × SDS loading buffer was added to the mixture, and boiled for 5 min at 95 °C.

2.6. RNA interference

Two Myo7a siRNAs were designed based on the mouse Myo7a cDNA sequence: CAGAGTCATTCTCCTCCAGAA and CCAGGTGTTCTT CATGAAGAA. An irrelevant siRNA sequence CGAGUGGUCUAGUUG AGAA was used as control. To examine the silencing efficiency of Myo7a siRNA, B16 cells were transfected with synthetic siRNA or control siRNA (QIAGEN, Hilden, Germany) at a final concentration of 100 nM using Lipofectamine RNAiMAX (Invitrogen, Carlsbad, CA) as described by the manufacturer.

2.7. Generation of mutations

Point mutants were generated using the QuickChange XL Site-Directed Mutagenesis Kit (Stratagene). Myo7a siRNA-resistant mutant is a siRNA-2-resistant Myo7a G5826C/C5829T mutant.

2.8. Cell adhesion and spreading assays

For cell adhesion, non-treated 48-well plates (Corning Costar Corp., Tewksbury, MA) were coated with 100 μl of 6 μg/ml Vitronectin (VN) (Merck KGaA, Darmstadt, Germany), Fibronectin (FN) (Merck KGaA, Darmstadt, Germany) or type I collagen (Sigma–Aldrich, St. Louis, MO) overnight at 4 °C. 1% Heat-denatured BSA was applied to block non-specific adhesion at 37 °C for 1 h. 300 μl of cell suspension were seeded into the wells in triplicate at 5×10^4 cells/well in cell adhesion buffer (RPMI 1640, 2 mM $CaCl_2$, 1 mM $MgCl_2$, 0.2 mM $MnCl_2$ and 0.5% BSA) and allowed to attach for 30 min at 37 °C. After careful washing with adhesion buffer to remove non-bound cells, WST-1 (Beyotime Institute of Biotechnology, Shanghai, China), a water-soluble tetrazolium salt for MTT Assays, was used to quantify the number of cells attached. The morphology of cells during the spreading was analyzed at 30-min time points. Adherent cells were treated with 4% formaldehyde for 15 min and typically 15 microscopic fields were randomly chosen to be photographed and analyzed.

For visualization of filopodia and quantification of filopodia length, B16 cells were co-transfected with Myo7a siRNA and Flag-Myo7a WT or Flag-Myo7a siRNA resistant mutant, and replated on VN 48 h after transfection. The quantification of filopodia length was performed as described previously. In brief, cells were selected randomly and all eligible filopodia of selected cells were measured with Slidebook 6. About 100 cells were measured for each condition in each experiment, and displayed data are representative of three experiments. Statistical evaluation for filopodia length was performed with software GraphPad Prism 5.

2.9. Transwell migration assays

Haptotactic cell migration assays were performed using Transwell chambers (Corning Costar Corp., Tewksbury, MA) with 8.0 μm pore size. The lower surface of Transwell membranes were coated with FN (10 μg/ml) at 37 °C for 1 h. 48 h After transfection 5×10^4 cells were seeded on the top of the Transwell membranes in the presence or absence of anti-integrin αvβ5 mAb P1F6 (Chemi-Con, Rosemont, Illinois) followed by 6 h incubation at 37 °C in RPMI 1640 with 2 mM $CaCl_2$, 1 mM $MgCl_2$, 0.2 mM $MnCl_2$ and 0.5% BSA. The Transwell membrane was then fixed with 4% formaldehyde for 15 min and stained by crystal violet. Typically 15 microscopic fields were randomly chosen for analyses.

2.10. Statistical analysis

All experiments were repeated for three times, and data were presented as means ± SD. Comparisons between two groups were made using unpaired *t*-test. Differences among more than two groups were compared using one-way ANOVA. *P* value less than 0.05 was considered as statistically significant.

3. Results

3.1. Myo7a directly interacts with integrin β5 cytoplasmic domain

Myo7a contains FERM domains in its tail (Fig. 1A), which has been known to determine the cellular localization and function in a variety of integrin-interacting proteins, and that gives us a hint about how Myo7a exerts its biological functions. To examine this hypothesis, purified Glutathione S-transferase (GST)-integrin β1, integrin β3 or integrin β5 cytoplasmic domain fusion proteins were incubated with total lysates from COS-7 cells transfected with

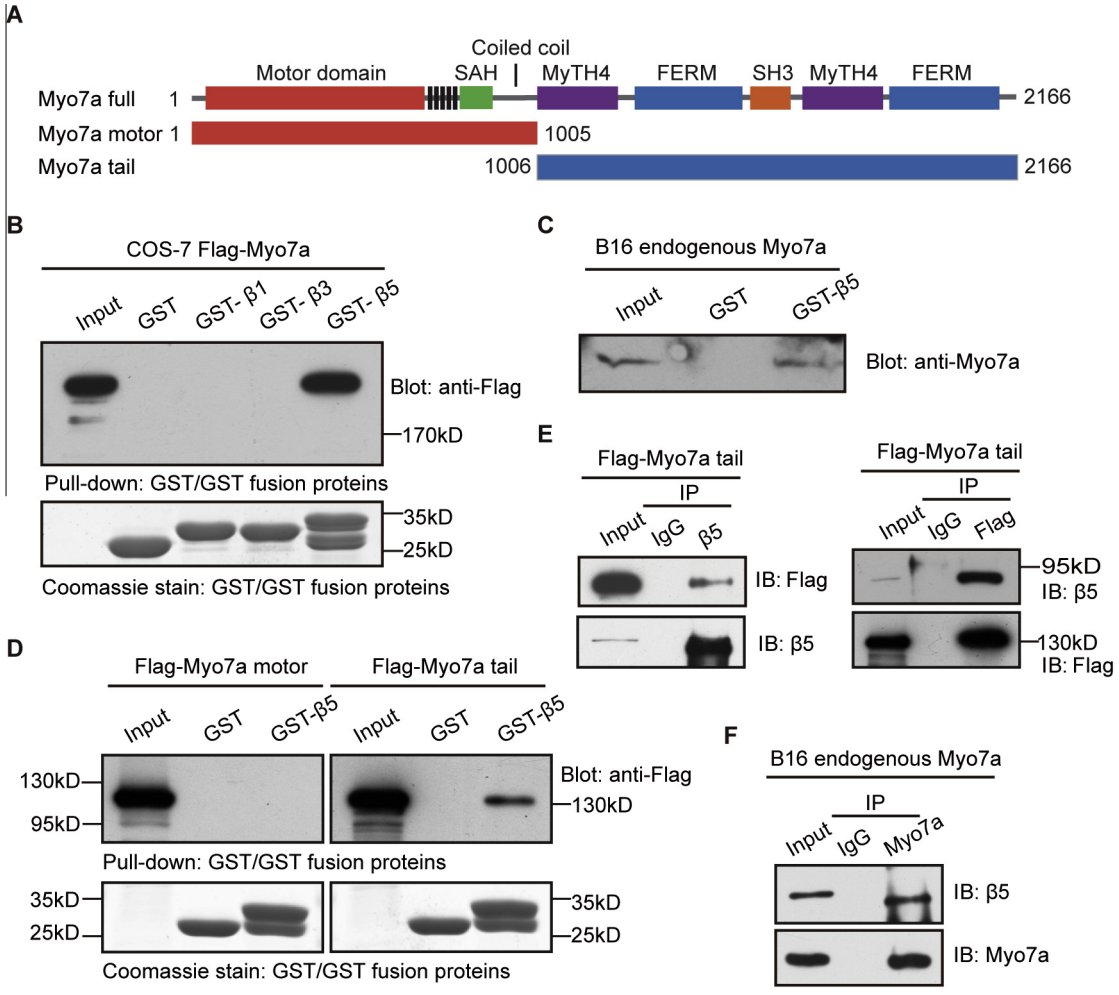

Fig. 1. Myo7a interacts with the integrin β5 subunit. (A) Sectioned bar diagram depicts the domain structure of Myo7a full, Myo7a motor and Myo7a tail. (B) Purified GST-β1, GST-β3 and GST-β5 cytoplasmic domain fusion protein were used to pull down Flag-Myo7a expressed in COS-7 cells, with GST alone as control. The left lane shows the input lysate containing Flag-Myo7a. (C) GST-β5 cytoplasmic domain fusion protein was used to pull down endogenous Myo7a in B16 cells. (D) Myo7a tail domain but not motor interacted directly with integrin β5 in a GST pull-down assay. (E) Myo7a tail domain associates with integrin β5 in Co-IP assays. B16 cells were transfected with Flag-tagged Myo7a tail. 48 h after transfection, cell lysates were immunoprecipitated with an anti-integrin β5 antibody and an anti-Flag antibody followed by immunoblotting using an anti-Flag antibody and an anti-integrin β5. 10 μg cell lysates containing Flag-Myo7a tail were loaded as input. (F) The interaction between endogenous Myo7a and integrin β5 in B16 cells was analyzed in a Co-IP assay.

Flag-tagged Myo7a in GST pull-down assays. We detected an interaction between Myo7a and GST-β5 cytoplasmic domain (Fig. 1B). In this study, we identified that Myo7a was highly expressed in B16 cells (Supplementary Fig. 1). Herein, endogenous Myo7a in mouse melanoma B16 cells was pulled down by GST-fused integrin β5 cytoplasmic domain (Fig. 1C). To map the binding regions between Myo7a and integrin β5, Myo7a was roughly divided into two regions: the N-terminal motor region, including 1–1018 aa which contains motor domain and neck region, and the C-terminal tail region, including 1006–2166 aa which contains MyTH4, SH3 and FERM domains (Fig. 1A). GST pull-down experiment showed that Myo7a tail, but not the N-terminal motor region, could interact with integrin β5 (Fig. 1D). Furthermore, Co-IP assays were performed to identify that Myo7a tail interacted with endogenous

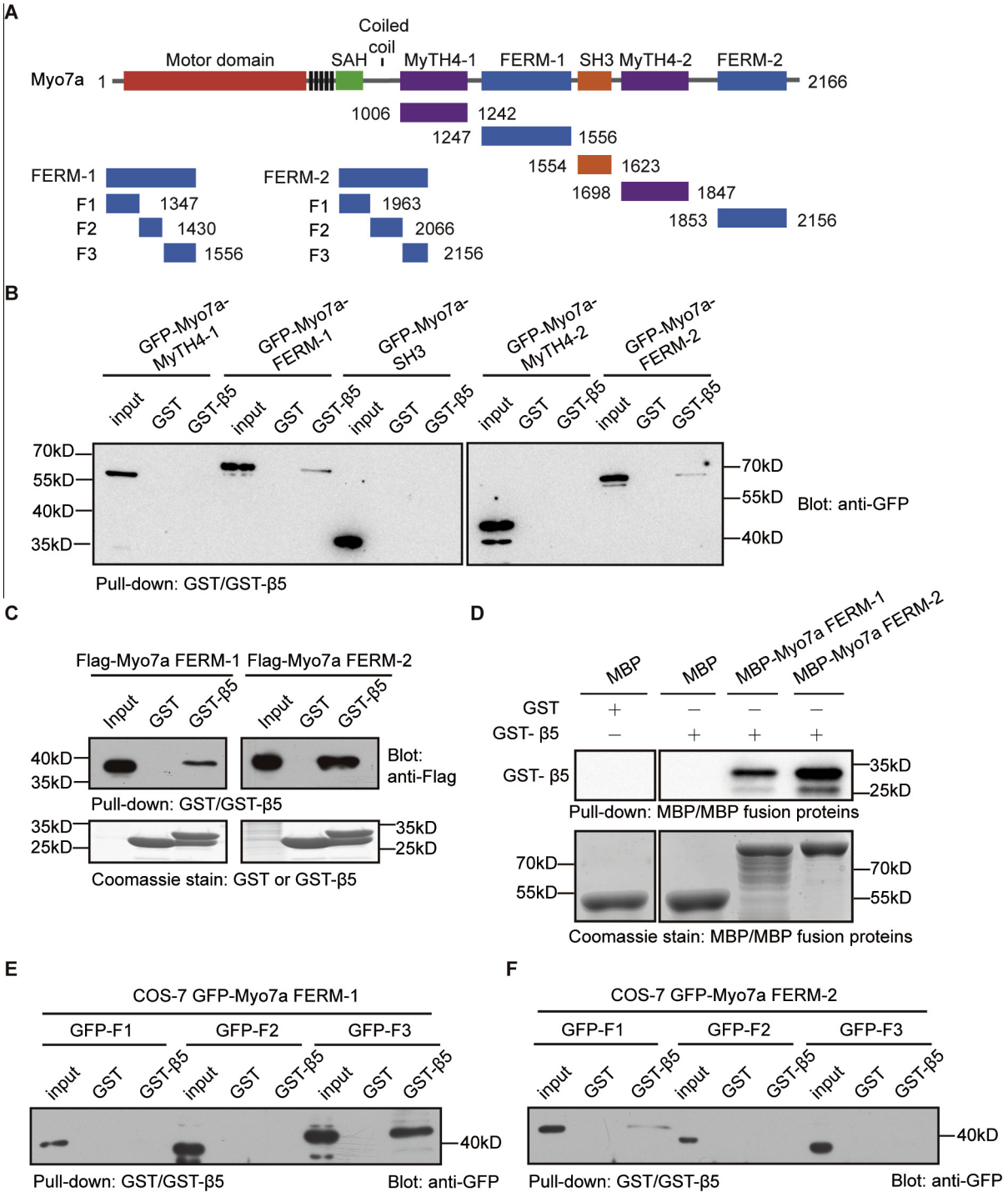

Fig. 2. Mapping of the integrin β5-binding region in the Myo7a tail. (A) Schematic illustration of the Myo7a structure and precise amino acid boundaries for each domain of Myo7a. (B) Various regions of the Myo7a tail were cloned into vector pEGFP and then were transfected into COS-7 cells. Myo7a FERM-1 and FERM-2 domains are associated with integrin β5 in COS-7 cells, as examined in a GST pull-down assay. (C) Flag-tagged Myo7a FERM-1 and FERM-2 domains were also interacted with integrin β5 in COS-7 cells. (D) Fusion protein MBP-Myo7a FERM-1 and MBP-Myo7a FERM-2 were incubated with GST-integrin β5 in vitro for MBP pull-down assay. Affinity matrices for MBP-tag were used. F1 subdomain of Myo7a FERM-1 domain (E) and F3 subdomain of Myo7a FERM-2 domain (F) interacted directly with integrin β5 cytoplasmic domain in a GST pull-down assay. 10 μg cell lysates were loaded as input.

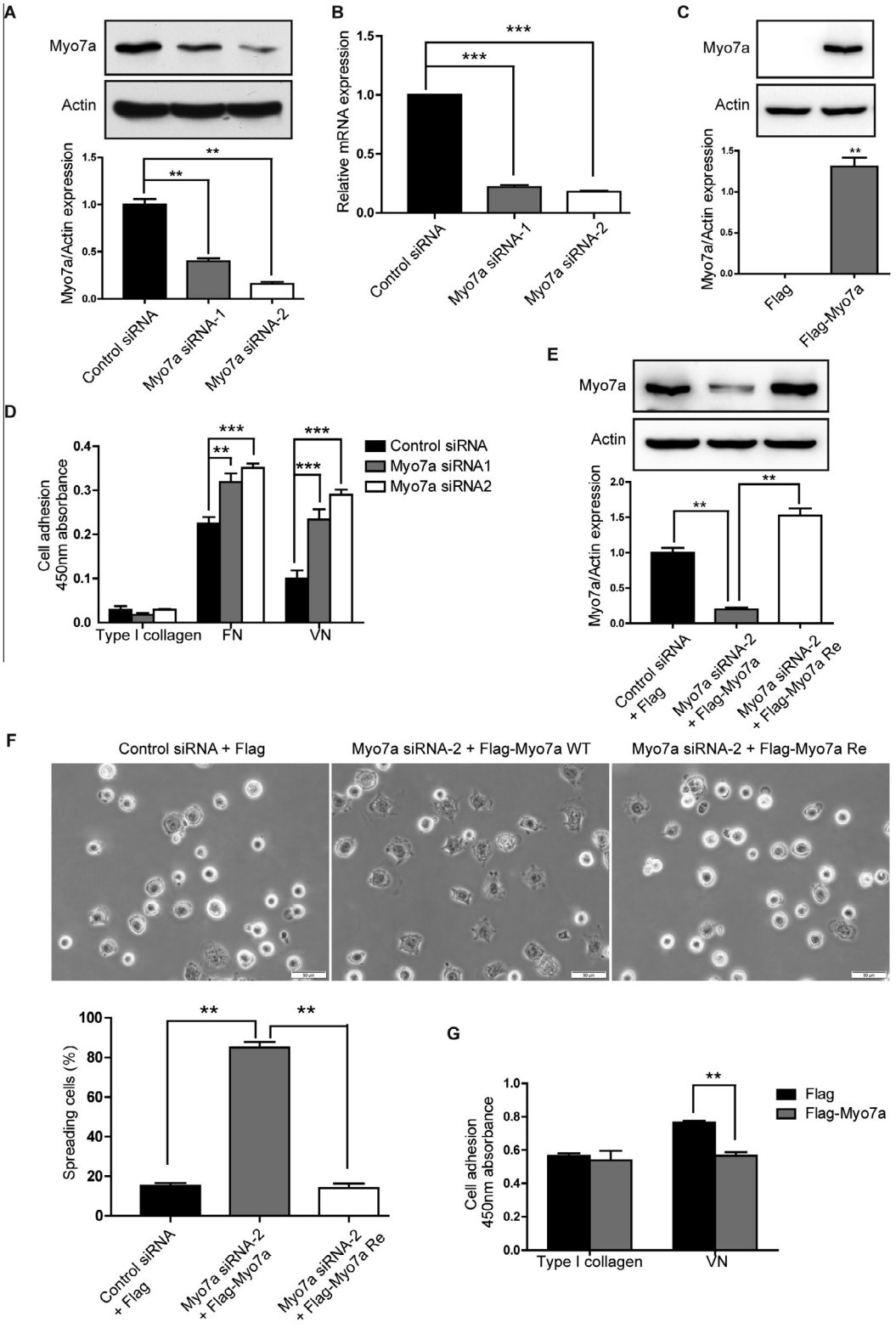

Fig. 3. Myo7a regulates integrin αvβ5-mediated cell spreading and adhesion Western blot assays (A) and Real-time qPCR (B) were performed to detect the efficiency of Myo7a knockdown by two Myo7a-specific siRNAs in B16 cells. $^{**}P < 0.01$; $^{***}P < 0.001$. (C) Western blot assays show the expression level of Myo7a in Myo7a-transfected MCF-7 cells. (D) Knockdown of Myo7a promotes cell adhesion on FN and VN. Attachment of Myo7a knockdown B16 cells on collagen type I, FN and VN (6 μg/ml) was analyzed at 30- and 60-min time points as three independent experiments. $^{**}P < 0.01$; $^{***}P < 0.001$. (E) The expression level of Myo7a of the above mentioned cells was examined by Western blot. Data are expressed as mean ± SD of three independent experiments, $^{**}P < 0.01$. (F) Flag-Myo7a WT or Flag-Myo7a siRNA-2-resistant mutant was transfected into control or siRNA-2 treated B16 cells. Cell spreading assays showed the different phenotypes of cells with different treatments. Top panel: representative images show spreading phenotypes of cells on VN (6 μg/ml) at 30-min time points. Scale bar: 50 μm. Lower panel shows quantitative analysis of the above images. $^{**}P < 0.01$. (G) Overexpression of Myo7a decreases cell adhesion on VN. Attachment of Myo7a overexpressed MCF-7 cells on type I collagen and VN (6 μg/ml) was analyzed at 30- and 60-min time points as three independent experiments. $^{**}P < 0.01$.

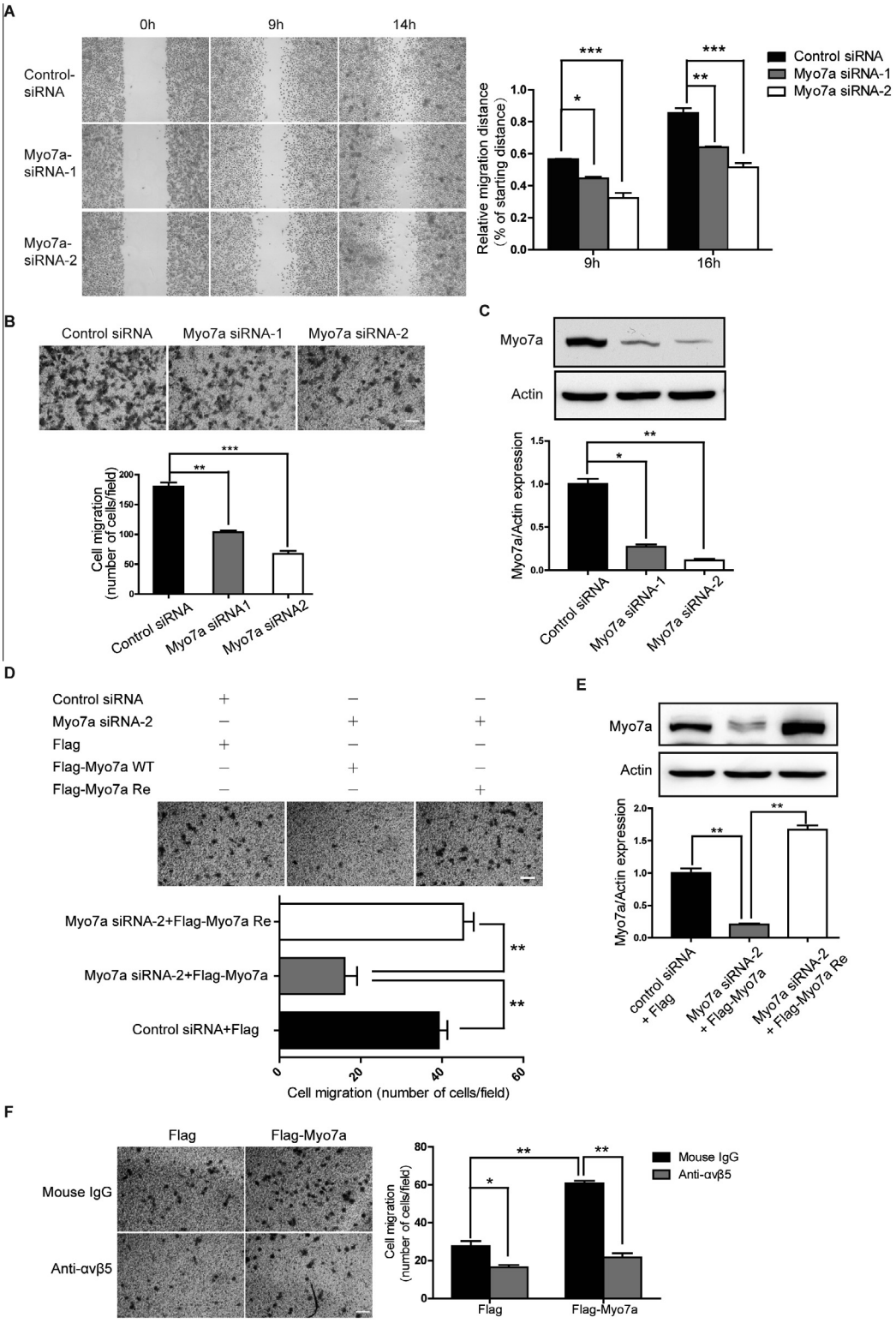

Fig. 4. Myo7a stimulates integrin αvβ5-mediated cell migration. (A) Knockdown of Myo7a suppresses B16 cell migration in wound healing assay. Left panel shows representative cell pictures 9 h ($^{*}P < 0.05$; $^{***}P < 0.001$) and 14 h ($^{**}P < 0.01$; $^{***}P < 0.001$) after scratching, and right panel shows quantitative analysis of cell migration. (B) Knockdown of Myo7a inhibits B16 cell migration in a Transwell migration assay. Top panel: crystal violet staining in a Transwell migration assay. Scale bar: 100 μm; bottom panel: quantitative analysis of cell migration. $^{**}P < 0.01$; $^{***}P < 0.001$. (C) The efficiency of Myo7a knockdown in B16 cells was examined by Western blot. Data are expressed as mean ± SD of three independent experiments, $^{*}P < 0.05$, $^{**}P < 0.01$. (D) B16 cells co-transfected with Myo7a siRNA-2 and Myo7a siRNA-2 siRNA resistant mutant restored the ability of cell migration. $^{**}P < 0.01$. (E) The transfection efficiency in the above mentioned cells was determined by Western blot. Data are expressed as mean ± SD of three independent experiments, $^{**}P < 0.01$. (F) MCF-7 cells transiently transfected with Flag-tagged Myo7a and empty Flag vector were analyzed for haptotactic cell migration towards VN in the presence or absence of normal mouse IgG and functional blocking anti-αvβ5 mAbs. Scale bar: 100 μm. Top panel shows representative images in crystal violet staining and lower panel shows quantitative analysis of cell migration. $^{*}P < 0.05$; $^{**}P < 0.01$.

integrin β5 in B16 cells (Fig. 1E). Importantly, the interaction between endogenous Myo7a and integrin β5 in B16 cells was found by Co-IP (Fig. 1F). These results indicated that Myo7a is a novel integrin-interacting protein through its tail region.

3.2. Integrin β5 subunit interacts with FERM domain of Myo7a tail

To determine the binding regions within Myo7a tail that bind integrin β5 cytoplasmic domain, we generated five constructs encoding various regions of the Myo7a tail as shown in Fig. 2A. We found that the integrin-binding regions located at the two FERM domains within Myo7a tail in a GST pull-down assay (Fig. 2B). Moreover, we constructed Flag-tagged Myo7a FERM domains and further determined the interaction region between Myo7a FERM domains and integrin β5 cytoplasmic domain (Fig. 2C). To rule out the possibility that an adapter protein is mediating the interaction between Myo7a tail and the cytoplasmic tail of integrin β5, we constructed MBP-tagged Myo7a FERM1/2 domains and purified the MBP–FERM fusion proteins, then incubated the proteins with purified GST-integrin β5. Results showed that the tail regions of Myo7a interact directly with integrin β5 cytoplasmic tail (Fig. 2D). Since each FERM domain is composed of three subdomains, F1, F2 and F3, we further mapped the distinct subdomains which mediated the interaction in a GST pull-down assay. Taken together, we identified that F3 of the first FERM domain and F1 of the second FERM domain interacted with integrin β5 cytoplasmic domain (Fig. 2E and F).

3.3. Myo7a inhibits integrin αvβ5-mediated cell adhesion

Given the aforementioned finding that Myo7a interacts with integrin β5 cytoplasmic domain, we continued to examine the potential role of Myo7a in αvβ5-mediated cell adhesion. Two Myo7a-specific siRNAs were synthesized and found to significantly inhibit the endogenous Myo7a expression in B16 cells (Fig. 3A and B). As shown in Fig. 3D, knockdown of Myo7a markedly promoted cell adhesion on VN, but not integrin β1-mediated cell adhesion on type I collagen. It was known that both integrin αvβ3 and αvβ5 participate in cell attachment and migration towards VN [17], and integrin αvβ3 usually serves as VN receptor in most cell lines. To elucidate the effects of Myo7a on αvβ5-mediated cell adhesion, we overexpressed Myo7a in MCF-7 cells (Fig. 3C), which express αvβ5 but not αvβ3 [18]. Intriguingly, we observed that B16 cells with Myo7a knockdown displayed well-spread morphology with obvious protrusions on the cell surface compared with control cells after cell adhesion for 30 min. This effect was specific as transfection of a mutant construct, which is resistant to Myo7a siRNA-2 knockdown (Supplementary Fig. 2), notably decreased the percentage of spread cells. Quantitative analysis showed that the spreading cells accounted for more than 80% of cells with Myo7a knockdown, whereas less than 25% of spreading cells were observed after restoring the expression of Myo7a (Fig. 3F). In addition, filopodia in Myo7a siRNA2 resistance cells were longer than the cells with Myo7a knockdown (Supplementary Fig. 3), suggesting that Myo7a was involved in the maintenance of filopodia. Fig. 3E showed the expression level of Myo7a of the above mentioned cells. As expected, overexpression of Myo7a in MCF-7 cells, lacking integrin αvβ3, inhibited cell adhesion on VN compared with the control group (Fig. 3G). Taken together, these results indicated that Myo7a inhibited cell spreading and adhesion in MCF-7 cells is mediated by integrin αvβ5.

3.4. Myo7a promotes integrin αvβ5-mediated cell migration

Given that cell adhesion is prerequisite for cell migration, we attempted to examine whether Myo7a affected cell migration on VN. To test this hypothesis, confluent monolayers of B16 cells transfected with Myo7a siRNAs and control siRNA were scratched, and then the cell mobility were observed at different time points (0 h, 9 h and 14 h). The results demonstrated that knockdown of Myo7a diminished the velocity of wound healing in B16 cells (Fig. 4A). Moreover, we performed the Transwell migration assay to examine the effect of Myo7a on cell migration, and the results showed that knockdown of Myo7a significantly inhibited B16 cell migration towards VN (Fig. 4B). The efficiency of Myo7a knockdown was examined by Western blot (Fig. 4C). To further validate the effect of Myo7a on cell migration, B16 cells co-transfected with Myo7a siRNA-2 and Myo7a siRNA-2 resistant mutant restored the ability of cell migration (Fig. 4D). As shown in Fig. 4E, the transfection efficiency was quantified by Western blot. Furthermore, as shown in Fig. 4F, MCF-7 cells were transfected with Flag-Myo7a or empty Flag vector, and overexpression of Flag-Myo7a markedly promoted cell migration towards VN. Importantly, Flag-Myo7a-induced cell migration could be blocked by a functional blocking anti-αvβ5 mAb (Fig. 4F). Collectively, these data indicated that Myo7a promoted integrin αvβ5-mediated cell migration.

4. Discussion

In the present investigation, we delineate previously unknown integrin-binding capacity for Myo7a and identified its role in non-stereocilia cell adhesion and migration. Previous studies have demonstrated that Myo7a were functionally correlated with inherited hearing loss. To date, several Myo7a-interacting proteins have been identified to play critical roles in maintaining the structure of stereocilia in the inner ear. The FERM domain of Myo7a had been identified to interact with transmembrane protein vezatin in a yeast two-hybrid screen, which is a ubiquitous protein of adherens cell–cell junctions [19]. In addition, harmonin, a PDZ domain-containing protein, interacts directly with Myo7a, and is absent from the disorganized hair bundles of *myosin VIIA* mutant mice [20]. Rzadzinska et al. found that interaction between Myo7a and twinfilin-2 is responsible for the establishment and maintenance of staircase-like organization of the stereocilia bundle and that interplay between complexes of Myo7a/twinfilin-2 is responsible for stereocilia length gradation within the bundle staircase [21]. In the present report, we identified a novel interaction between FERM domain-containing motor molecule Myo7a and integrin β5 cytoplasmic tail (Fig. 1B). For the first time we established a new connection between Myo7a and ECM through binding to integrin. Furthermore, we mapped that the cytoplasmic tail of integrin β5 binds to F3 subdomain of the first FERM domain and F1 subdomain of the second FERM domain at the C-terminus of Myo7a (Fig. 2D and E). Interestingly, Rzadzinska et al. pointed out that exogenous expression of Myo7a in BHK-21 fibroblast cells results in a reduced number of filopodia, the amount of Myo7a in the cell cytoplasm correlates with the number of actin filled cellular protrusion and higher levels of Myo7a in the cell cytoplasm strongly correlate with filopodia suppression [21]. These findings suggested that overexpressed cytoplasmic Myo7a interact with integrins, e.g., αvβ5 and connects with the ECM. Thus, more Myo7a are not favorable for the formation of filopodia, resulting in less filopodia in number and shorter filopodia in length. In our work, we identified that Myo7a regulates cell adhesion and migration through integrin αvβ5. We found that knockdown of endogenous Myo7a in B16 cells by RNAi promotes cell spreading, adhesion and inducing protrusions at the peripheral of cells (Fig. 3F and Supplementary Fig. 2), suggesting that knockdown of Myo7a may facilitate the initiation of filopodia since reduced cell-matrix contact favors the formation of protrusion at this stage. However, our data also demonstrated that filopodia in cells expressing

Myo7a siRNA-2-resistant construct were longer than filopodia of cells with Myo7a knockdown (Supplementary Fig. 3), suggesting that Myo7a is involved in the maintenance of the length of filopodia, probably by formation of tip complexes with integrin αvβ5 or twinfilin-2. Therefore, if Myo7a could complex with integrin αvβ5 and twinfilin-2 at the tips of stereocilia to regulate the length gradation warrants future investigations.

We previously found that p21-activated kinase 4 (PAK4) interacts with the integrin β5 cytoplasmic domain and regulates αvβ5-mediated breast cancer cell migration [14]. These findings suggested that integrin αvβ5 plays an important role in the regulation of cell migration. Integrin β5 has been reported to contribute to the tumorigenesis of breast cancer cells [22]; meanwhile recent study showed that Myo10 was required for breast cancer cell invasion and dissemination by association with mutant p53 [23]. These related findings raised an important question that whether Myo7a plays a role in tumor progression *via* interaction with integrin β5. However, evidence for the role of Myo7a in tumor progression remains elusive.

In summary, we identified that Myo7a is a novel integrin β5-interacting protein. By interaction with integrin, we pointed out that Myo7a is linked to the ECM. Myo7a plays a role in regulating integrin αvβ5-mediated cell adhesion and migration in non-stereocilia cells, a finding that expanded our current knowledge on Myo7a. The identification of Myo7a-integrin β5 interaction may shed light on the deeper understanding of the role of Myo7a in the progression of hereditary deafness and maintenance of the structural integrity of stereocilia in the inner ear.

Acknowledgments

This work was supported by grants from the Ministry of Science and Technology of China 2013CB910501, 2010CB912203 and 2010CB529402, the National Natural Science Foundation of China 81230051, 30830048, 31170711 and 81321003, the 111 Project of the Ministry of Education, Beijing Natural Science Foundation 7120002 and Peking University grants BMU20120314 and BMU20130364, and a Leading Academic Discipline Project of Beijing Education Bureau to H.Z.

Appendix A. Supplementary data

Supplementary data associated with this article can be found, in the online version, at http://dx.doi.org/10.1016/j.febslet.2014.06.049.

References

[1] Hynes, R.O. (2002) Integrins: bidirectional, allosteric signaling machines. Cell 110, 673–687.
[2] Humphries, M.J. (2000) Integrin structure. Biochem. Soc. Trans. 28, 311–339.
[3] Hartman, M.A., Finan, D., Sivaramakrishnan, S. and Spudich, J.A. (2011) Principles of unconventional myosin function and targeting. Annu. Rev. Cell Dev. Biol. 27, 133–155.
[4] L.M. Coluccio, SpringerLink (Online service), Myosins a superfamily of molecular motors, in: Proteins and Cell Regulation, vol. 7, Springer, Dordrecht, 2008, pp. xii, 475 p., 417 p. of plates.
[5] Weil, D., Blanchard, S., Kaplan, J., Guilford, P., Gibson, F., Walsh, J., Mburu, P., Varela, A., Levilliers, J., Weston, M.D., et al. (1995) Defective myosin VIIA gene responsible for Usher syndrome type 1B. Nature 374, 60–61.
[6] Weil, D., Kussel, P., Blanchard, S., Levy, G., Levi-Acobas, F., Drira, M., Ayadi, H. and Petit, C. (1997) The autosomal recessive isolated deafness, DFNB2, and the Usher 1B syndrome are allelic defects of the myosin-VIIA gene. Nat. Genet. 16, 191–193.
[7] Tamagawa, Y., Ishikawa, K., Ishida, T., Kitamura, K., Makino, S., Tsuru, T. and Ichimura, K. (2002) Phenotype of DFNA11: a nonsyndromic hearing loss caused by a myosin VIIA mutation. Laryngoscope 112, 292–297.
[8] Mburu, P., Liu, X.Z., Walsh, J., Saw Jr., D., Cope, M.J., Gibson, F., Kendrick-Jones, J., Steel, K.P. and Brown, S.D. (1997) Mutation analysis of the mouse myosin VIIA deafness gene. Genes Funct. 1, 191–203.
[9] Chishti, A.H., Kim, A.C., Marfatia, S.M., Lutchman, M., Hanspal, M., Jindal, H., Liu, S.C., Low, P.S., Rouleau, G.A., Mohandas, N., Chasis, J.A., Conboy, J.G., Gascard, P., Takakuwa, Y., Huang, S.C., Benz Jr., E.J., Bretscher, A., Fehon, R.G., Gusella, J.F., Ramesh, V., Solomon, F., Marchesi, V.T., Tsukita, S., Hoover, K.B., et al. (1998) The FERM domain: a unique module involved in the linkage of cytoplasmic proteins to the membrane. Trends Biochem. Sci. 23, 281–282.
[10] Pearson, M.A., Reczek, D., Bretscher, A. and Karplus, P.A. (2000) Structure of the ERM protein moesin reveals the FERM domain fold masked by an extended actin binding tail domain. Cell 101, 259–270.
[11] Campbell, I.D. and Ginsberg, M.H. (2004) The talin–tail interaction places integrin activation on FERM ground. Trends Biochem. Sci. 29, 429–435.
[12] Harburger, D.S., Bouaouina, M. and Calderwood, D.A. (2009) Kindlin-1 and -2 directly bind the C-terminal region of beta integrin cytoplasmic tails and exert integrin-specific activation effects. J. Biol. Chem. 284, 11485–11497.
[13] Zhang, H., Berg, J.S., Li, Z., Wang, Y., Lang, P., Sousa, A.D., Bhaskar, A., Cheney, R.E. and Stromblad, S. (2004) Myosin-X provides a motor-based link between integrins and the cytoskeleton. Nat. Cell Biol. 6, 523–531.
[14] Zhang, H., Li, Z., Viklund, E.K. and Stromblad, S. (2002) P21-activated kinase 4 interacts with integrin alpha v beta 5 and regulates alpha v beta 5-mediated cell migration. J. Cell Biol. 158, 1287–1297.
[15] Belyantseva, I.A., Boger, E.T., Naz, S., Frolenkov, G.I., Sellers, J.R., Ahmed, Z.M., Griffith, A.J. and Friedman, T.B. (2005) Myosin-XVa is required for tip localization of whirlin and differential elongation of hair-cell stereocilia. Nat. Cell Biol. 7, 148–156.
[16] Yu, Y., Wu, J., Wang, Y., Zhao, T., Ma, B., Liu, Y., Fang, W., Zhu, W.G. and Zhang, H. (2012) Kindlin 2 forms a transcriptional complex with beta-catenin and TCF4 to enhance Wnt signalling. EMBO Rep. 13, 750–758.
[17] Wayner, E.A., Orlando, R.A. and Cheresh, D.A. (1991) Integrins alpha v beta 3 and alpha v beta 5 contribute to cell attachment to vitronectin but differentially distribute on the cell surface. J. Cell Biol. 113, 919–929.
[18] Brooks, P.C., Klemke, R.L., Schon, S., Lewis, J.M., Schwartz, M.A. and Cheresh, D.A. (1997) Insulin-like growth factor receptor cooperates with integrin alpha v beta 5 to promote tumor cell dissemination in vivo. J. Clin. Investig. 99, 1390–1398.
[19] Kussel-Andermann, P., El-Amraoui, A., Safieddine, S., Nouaille, S., Perfettini, I., Lecuit, M., Cossart, P., Wolfrum, U. and Petit, C. (2000) Vezatin, a novel transmembrane protein, bridges myosin VIIA to the cadherin–catenins complex. EMBO J. 19, 6020–6029.
[20] Boeda, B., El-Amraoui, A., Bahloul, A., Goodyear, R., Daviet, L., Blanchard, S., Perfettini, I., Fath, K.R., Shorte, S., Reiners, J., Houdusse, A., Legrain, P., Wolfrum, U., Richardson, G. and Petit, C. (2002) Myosin VIIa, harmonin and cadherin 23, three Usher I gene products that cooperate to shape the sensory hair cell bundle. EMBO J. 21, 6689–6699.
[21] Rzadzinska, A.K., Nevalainen, E.M., Prosser, H.M., Lappalainen, P. and Steel, K.P. (2009) MyosinVIIa interacts with Twinfilin-2 at the tips of mechanosensory stereocilia in the inner ear. PLoS One 4, e7097.
[22] Bianchi-Smiraglia, A., Paesante, S. and Bakin, A.V. (2013) Integrin beta5 contributes to the tumorigenic potential of breast cancer cells through the Src-FAK and MEK-ERK signaling pathways. Oncogene 32, 3049–3058.
[23] Arjonen, A., Kaukonen, R., Mattila, E., Rouhi, P., Hognas, G., Sihto, H., Miller, B.W., Morton, J.P., Bucher, E., Taimen, P., Virtakoivu, R., Cao, Y., Sansom, O.J., Joensuu, H. and Ivaska, J. (2014) Mutant p53-associated myosin-X upregulation promotes breast cancer invasion and metastasis. J. Clin. Investig.